Optimization of fiber distribution in fiber reinforced composite by using NURBS functions

Hamid Ghasemi[1], Roberto Brighenti[2], Xiaoying Zhuang[3], Jacob Muthu[4],Timon Rabczuk*[1, 5]

[1] Institute of Structural Mechanics, Bauhaus University Weimar, Marienstraße 15, 99423 Weimar,Germany
[2] Dep. of Civil Eng, Env. & Architect. , U of Parma, Parco Area delle Scienze, 181/A, 43100 Parma, Italy
[3] Dep. of Geotech. Eng., College of Civil Eng., Tongji Uni., 1239 Siping Road, Shanghai 200092, China
[4] School of Mechanical, Industrial and Aeronautical Eng., U. of the Witwatersrand, WITS 2050, S. Africa
[5] Professor at School of Civil, Environmental and Architectural Eng., Korea University, Seoul, S. Korea

Abstract

This research deals with the optimization of short fibers distribution in continuum structures made of Fiber Reinforced Composite (FRC) by adopting an efficient gradient based optimization approach. Motivated by lack of non-heuristic and mesh independent optimization algorithm to obtain the optimum distribution of short fibers through a design domain, Non-Uniform Rational B-spline (NURBS) basis functions have been implemented to define continuous and smooth mesh independent fiber distribution function as well as domain discretization. Thanks to higher order (here quadratic) NURBS basis functions along with their compact support, a drastic reduction in computational time has been obtained by increasing mesh size while the accuracy of the model is maintained. Moreover combination of NURBS with sensitivity based optimization method allows a fast convergence to optimum fiber distribution layout. Minimization of elastic strain energy and maximization of fundamental frequency have been considered as objective functions for static and free vibration problems, respectively; to get the maximum fiber exploitation in the structural element. Nodal volume fraction of fiber was defined as the optimization design variable while a homogenization approach based on the random orientation of short fibers in the matrix has been adopted. Some numerical examples related to the structural response under static loading as well as the free vibration behavior are finally conducted to demonstrate the capability and reliability of the model.

Keywords: Fiber Reinforced Composite (FRC), Fiber Distribution Optimization, Objective Function, NURBS, Optimization

---

*Corresponding Author: Tell: (+49)3643-584511, E-Mail: timon.rabczuk@uni-weimar.de

Nomenclature:

$\boldsymbol{B}_{i,j}$	Control points net
$\boldsymbol{C}(\xi)$	NURBS curve
$\boldsymbol{C}_f(\boldsymbol{x}), \boldsymbol{C}_m(\boldsymbol{x})$	Elastic tensor of the fiber and of the matrix material, respectively
$\boldsymbol{C}_{eq}$	Homogenized elastic tensor of the composite
$\boldsymbol{D}$	Elasticity matrix of a structure discretized with finite element
$\boldsymbol{E}_f, \boldsymbol{E}_m$	Young's modulus of the fiber phase and of the matrix, respectively
$\boldsymbol{f}$	System force vector
$\boldsymbol{i}$	Unit vector parallel to the generic fiber axis
$\boldsymbol{K}$	System stiffness matrix
$\boldsymbol{M}$	System mass matrix
$\boldsymbol{N}$	Matrix of shape functions
$\boldsymbol{N}_{i,p}(\xi), \boldsymbol{M}_{j,q}(\boldsymbol{\eta}), \boldsymbol{R}_i^p(\xi)$	NURBS and B-spline basis functions
$\boldsymbol{Q} = (\boldsymbol{i} \otimes \boldsymbol{i})$	Second-order tensor related to the fiber lying along the $\boldsymbol{k}$ direction
$\boldsymbol{S}(\xi, \boldsymbol{\eta})$	NURBS surface
$\boldsymbol{u}$	System displacement vector
$\boldsymbol{U}, \boldsymbol{U}^i$	Total strain energy and elastic strain energy for i^{th} load case
$\boldsymbol{V}, \boldsymbol{V}_m, \boldsymbol{V}_f$	Volume of the composite, volume of the matrix phase and volume of the fiber fraction present in the RVE, respectively
$\boldsymbol{w}'$	Composite work rate
$\boldsymbol{w}_i$	i^{th} weight
$\boldsymbol{w}_{f0}, \boldsymbol{w}_f$	Initial and total fiber weight at every iteration
$\boldsymbol{x}$	Generic position vector
$\boldsymbol{\varepsilon}, \dot{\tilde{\boldsymbol{\varepsilon}}}$	Strain and virtual strain rate tensors, respectively
$\boldsymbol{\varepsilon}_f, \widetilde{\boldsymbol{\varepsilon}_f}, \dot{\widetilde{\boldsymbol{\varepsilon}_f}}$	Fiber strain, virtual strain and virtual strain rate, respectively
$\boldsymbol{\kappa}(\boldsymbol{x})$	Point function denoting the presence of the matrix at the location **x**
$\boldsymbol{\chi}(\boldsymbol{x})$	Point function denoting the presence of the fiber at the location **x**
$\boldsymbol{\varphi}_{i,j}$	Nodal fiber volume fraction
$\boldsymbol{\lambda}_i$	Associated weight for strain energy
$\boldsymbol{\mu} = \frac{\boldsymbol{V}_m}{\boldsymbol{V}}$	RVE matrix volume fraction
$\boldsymbol{\eta}_p = \frac{\boldsymbol{V}_f}{\boldsymbol{V}}$	RVE fiber volume fraction of the fiber phase
$\boldsymbol{\eta}_p(\boldsymbol{x}, \boldsymbol{y})$	Fiber distribution function
$\boldsymbol{\rho}_m, \boldsymbol{\rho}_f, \boldsymbol{\rho}(\boldsymbol{x}, \boldsymbol{y})$	Matrix, fiber and equivalent density at every point in the design domain
$\boldsymbol{\psi}_1, \boldsymbol{\psi}_2$	Upper and lower bounds Lagrange multipliers
$\boldsymbol{\varpi}_i, \boldsymbol{\varpi}_{min}$	i^{th}eigenvalue and fundamental frequency
$\boldsymbol{\phi}_i$	Eigenvector associated with i^{th}eigenvalue
$\boldsymbol{\sigma}, \boldsymbol{\sigma}_f, \boldsymbol{\sigma}_{eq}$	Stress in composite, axial stress in a fiber and in the equivalent material

1. Introduction

Fiber Reinforced Composite (FRC) materials have been heavily investigated in the last decades and are widely used in advanced applications such as in aerospace, structural, military and transportation industries due to their elevated mechanical properties values to weight (or cost) ratio. Thanks to their excellent structural qualities like high strength, fracture toughness, fatigue resistance, light weight, erosion and corrosion resistance, a particular interest has been born not only in engineers for the use of FRCs in advanced industrial applications, but also in researchers to develop and optimize their particular and useful characteristics.

The general behavior of a FRC depends on the characteristics of the composite constituents such as fiber reinforcements, resin and additives; each of these constituents has an important role in the composite characteristics and such aspects have driven some researchers to combine them differently for obtaining enhanced materials. In the present work we have focused specifically on fibers distribution which has a critical role in enhancing structural load bearing capacity.

The mechanical properties of composites depend on many fiber's variables such as fiber's material, volume fraction, size and mesostructure. This latter aspect deals with fiber configuration, orientation, layout and dispersion. Available literatures aimed at the optimization of composite's performance with respect to the above mentioned fiber related variables, have been focused on improving specific performance of a classical laminated or Functionally Graded (FG) composites by changing the fiber's layout (ply orientation) or fiber volume fraction, by using heuristic optimization methods, especially the so-called Genetic Algorithm (GA) [1-7]. Salzar [8] tried to optimize a pressurized cylindrical pressure vessel by functionally grading the fiber volume fraction through the thickness of vessel. The work of Nadeau and Ferrari [9] addressed microstructural optimization of a FG layer subjected to thermal gradient, assuming that its parameters vary through the thickness of the layer; in their work the microstructure was characterized by fiber volume fraction, aspect ratio and orientation distribution. Honda and Narita [10] optimized vibration characteristics of a laminated structure by changing the orientation of fibers and intentionally providing local anisotropy; in their work fiber orientation angle and GA were implemented as design variable and optimization methodology respectively. Murugan and coworkers [11] performed optimization to minimize the in-plane stiffness and maximize the out of plane bending stiffness of a morphing skin used in aircraft wing made of laminate composite, by spatially varying the volume fraction of the fibers in the different layers; in particular the laminate was discretized through its thickness and equivalent material properties in each element were obtained based on homogenization technique using multi-scale constitutive model. Smooth particle hydrodynamics was implemented in Kulasegaram and Karihaloo works [12,13] in order to model and optimize short steel fibers distribution and orientation in self compacting concrete flow. Huang and Haftka [14] tried to optimize fibers orientation (not their distribution) near a hole in a single layer of multilayer composite laminates in order to increase the load caring capacity by using Genetic Algorithm (GA). Brighenti [15-17] used GA in his series of works on fiber distribution and patch repair optimization for cracked plates (to get the maximum exploitation of a given available patch element area by determining its best conformation around the cracked zone). The presence of the patch in a point of the structure is accounted for by properly modifying (i.e. increasing) the elastic modulus, similarly to what has been done with fiber distribution optimization in FRC material [18]. In particular the optimum distribution of the short fibers in a FRC, obtained by using GA, has been usually addressed in the literatures by assuming a constant value of the total fiber content, the optimum layout for fiber distribution has been determined in order to fulfill some given objective functions.

Computational cost is a very important aspect in optimization problem, particularly in industrial applications. Basically, the use of evolutionary algorithms, such as GA in [18], often leads to some limitations; in fact it is well-known as GA is problematic in some issues. Among them, its heuristic nature, high computational cost and sometimes the tendency to converge towards local optima instead of global optima – if proper so-called mutation strategies are not considered in the method – can be counted. In contrary with GA, gradient based methods which use gradient of the objective function evaluated with respect to design variables to find next direction in searching process (tending toward the optimum point), shows lots of merit particularly for complex geometries such as those often used in industrial applications.

There are also some limitations in using FE mapping of the fiber content [18] due to the element wise poor representation of the fiber layout: the first one is the possibility of mesh dependency for the results, since the final fibers arrangement resulting from the optimization is commonly determined based on fiber content of each finite element. Secondly, it could be easily understood that in order to have good layout representation, fine mesh and consequently costly computation should be done; moreover further post processing technique such as filtering or smoothing becomes necessary when this method is implemented. Thirdly, it must be also considered that, before economical and technological evaluations are performed, to fabricate element-wise variation of fiber content in a discretized continuum structure is still a daunting step with present available technologies. Fig. 1 schematically shows such limitations involved in FE mapping representation.

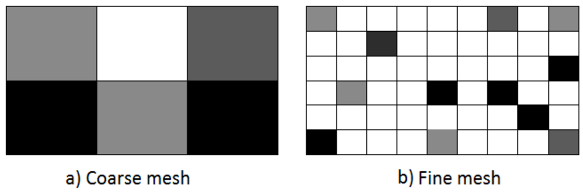

Fig.1. Schematic illustration of mesh dependency in element-based representation of fiber volume fraction

In this work instead of using element-based fiber volume fraction description, as has been already done in other literatures, the idea of utilizing quadratic NURBS basis functions in order to smoothly and continuously approximate given set of nodal points, has been developed. Promising characteristics of NURBS basis functions - such as compact support and higher order elements - not only provides mesh independent distribution results but also makes it possible to use coarse meshes to decrease computational time, while maintaining the accuracy of the results. The presented novel computational approach combines NURBS-based and gradient-based optimization methodologies to get an efficient optimization algorithm, which has been verified to be enough accurate, computationally fast and convenient for real industrial applications.

The paper is organized as follows: firstly homogenization technique for obtaining equivalent material property and then NURBS basis functions, derivatives, curve and surface representation are described in Sections 2 and 3; Section 4 defines the optimization problem while Sections 5 and 6 include some numerical examples with interpretation of the obtained results and summarizes the main concepts developed in this research, respectively.

2. FRC homogenization methodology

Basically the aim of homogenization techniques is to determine equivalent material characteristics in a Representative Volume Element (RVE) of composite material. There are some classical approaches in order to model the material properties of composites; among which the Rule of Mixture, Hashin-Shtrikman type bounds [19, 20], Variational Bounding Techniques [21], Self Consistency Method [22] and Mori-Tanaka Method [23] can be mentioned. The homogenization approach used in this research work is a simplified version of recently developed mechanical model (by the second author of this work [24]), to get the FRC constitutive behavior based on the shear stress distribution along the fiber-matrix interface during the loading process. The adopted model for fiber homogenization can be considered to be mechanically-based, since the fiber contribution to the FRC mechanical properties are determined from the effective stress transfer between matrix and fibers; moreover the possibility of fiber-matrix debonding can be easily taken into account. Since the goal of this paper is to focus on fiber distribution through the structure rather than developing micromechanical model, for sake of simplicity we neglect this issue in the present work. Moreover it can be declared that for not too high stressed composite elements (as followed in our numerical examples) leading to shear fiber-matrix interface stresses well below the allowable limit shear bimaterial stress, the debonding phenomenon can reasonably assumed not to occur as well as fiber breaking. This approach is briefly summarized below; however interested reader can refer to [24-26] for more details.

The equivalent elastic properties of a fiber reinforced composite material – for which the hypotheses of short, homogeneously and randomly dispersed fibers are made – can be obtained by equating the virtual work rate of constituents for a RVE (it is assumed that the RVE characteristic length *d* is much more lower that the structure characteristic length *D*) of the composite material (Fig.2) with equivalent homogenized one:

$$w' = \overbrace{\int_V \kappa(\boldsymbol{x})\, \dot{\tilde{\boldsymbol{\varepsilon}}} : \boldsymbol{\sigma} dV + \int_V \chi(\boldsymbol{x})\, \dot{\widetilde{\boldsymbol{\varepsilon}_f}} : \boldsymbol{\sigma_f}\, dV}^{composite's\ work\ rate} = \overbrace{\int_V \dot{\tilde{\boldsymbol{\varepsilon}}} : \boldsymbol{\sigma_{eq}} dV}^{homogenized\ material's\ work\ rate} \tag{1}$$

where $\dot{\tilde{\boldsymbol{\varepsilon}}}_{\mathbf{f}}$, $\boldsymbol{\sigma}_{\mathbf{f}}$ are the virtual strain rate and the stress in a fiber, respectively, while the scalar functions $\kappa(\mathbf{x})$, $\chi(\mathbf{x})$ assume the following meaning:

$$\kappa(\boldsymbol{x}) = \begin{cases} 1 & if\ (\boldsymbol{x}) \in V_m \\ 0 & if\ (\boldsymbol{x}) \notin V_m \end{cases} \quad \text{and} \quad \chi(\boldsymbol{x}) = \begin{cases} 1 & if\ (\boldsymbol{x}) \in V_f \\ 0 & if\ (\boldsymbol{x}) \notin V_f \end{cases} \tag{2}$$

and allow us to identify the location of the material point $\boldsymbol{x}$ either in the matrix or in the reinforcing phase.

The constitutive relationships of the fibers and of the bulk material can be simply expressed through the following linear relations:

$$\boldsymbol{\sigma_f} = E_f \cdot (\boldsymbol{i} \otimes \boldsymbol{i}) : \boldsymbol{\varepsilon} \quad \text{and} \quad \boldsymbol{\sigma_{eq}}(\boldsymbol{x}) = \boldsymbol{C_{eq}}(\boldsymbol{x}) : \boldsymbol{\varepsilon} \tag{3}$$

in which E_f is the fibers' Young's modulus, $\boldsymbol{\varepsilon_f}$ is the fiber strain, $\boldsymbol{C_{eq}}$ is the composite equivalent elastic tensor while $\boldsymbol{\varepsilon}$ is the actual matrix strain tensor. Eq. (3) has been written by taking into account that the matrix strain measured in the fiber direction is given by $\boldsymbol{\varepsilon_f} = (\boldsymbol{i} \otimes \boldsymbol{i}) : \boldsymbol{\varepsilon}$ where $\boldsymbol{i} = (sin\theta cos\phi\ sin\theta sin\phi\ cos\theta)$ is the unit vector identifying the generic fiber direction, (Fig.2) and analogously for the virtual $\widetilde{\boldsymbol{\varepsilon}_{\mathbf{f}}}$ and the virtual strain rate,

$$\widetilde{\boldsymbol{\varepsilon_f}} = (\boldsymbol{i} \otimes \boldsymbol{i}) : \tilde{\boldsymbol{\varepsilon}} \quad \text{and} \quad \dot{\widetilde{\boldsymbol{\varepsilon_f}}} = (\boldsymbol{i} \otimes \boldsymbol{i}) : \dot{\tilde{\boldsymbol{\varepsilon}}} \tag{4}$$

By substituting the above expressions in the virtual work rate equality (Eq. (1)) we can finally identify the composite equivalent elastic tensor:

$$\boldsymbol{C_{eq}}(\boldsymbol{x}) = \frac{1}{V} \int_V \{\kappa(\boldsymbol{x}) \cdot \boldsymbol{C_m} + \chi(\boldsymbol{x}) E_f \cdot [\boldsymbol{Q} \otimes \boldsymbol{Q}]\} dV =$$

$$= \mu \cdot \boldsymbol{C_m} + \eta_p E_f \cdot \int_V \boldsymbol{Q} \otimes \boldsymbol{Q}\, dV \tag{5}$$

where the second-order tensor $\boldsymbol{Q} = (\boldsymbol{i} \otimes \boldsymbol{i})$ has been introduced and the matrix and fiber volume fractions $\mu = \frac{1}{V} \int_V \kappa(\boldsymbol{x})\, dV = \frac{V_m}{V}$ and $\eta_p = \frac{1}{V} \int_V \chi(\boldsymbol{x})\, dV = \frac{V_f}{V}$ have been used.

It can be easily deduced as the equivalent material is macroscopically homogeneous at least at the scale of the RVE with volume V – i.e. the equivalent elastic tensor $\boldsymbol{C_{eq}}(\boldsymbol{x})$ does not depend on the position vector, i.e. $\boldsymbol{C_{eq}}(\boldsymbol{x}) = \boldsymbol{C_{eq}}$.

The calculation of the equivalent elastic tensor $\boldsymbol{C}_{eq}$ through Eq. (5), requires to evaluate the below integral over a sufficiently large volume, representative of the macroscopic characteristics of the composite. The above integral can be suitably assessed on a hemisphere volume which allows considering all possible fiber orientations in the composite:

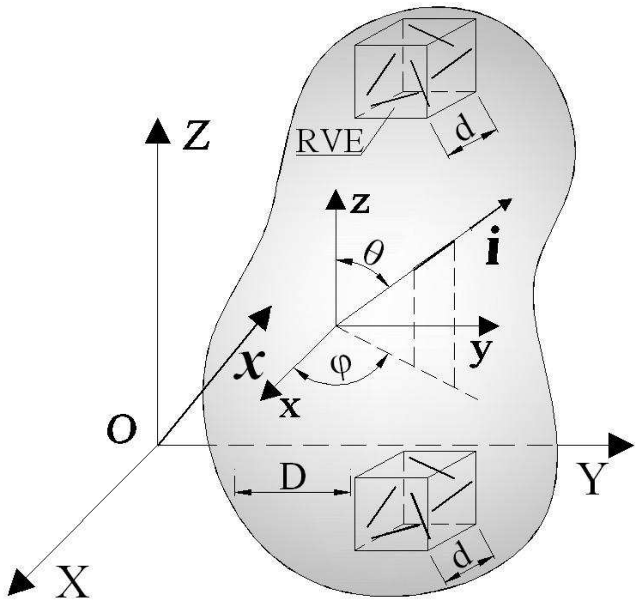

Fig.2. Fiber reinforced composite material: definition of the RVE (with a characteristic length d, while the composite has a characteristic length D>>d) and of the fiber orientation angles φ, θ, ref. [25]

$$\frac{1}{V_{hem}}\int_{V_{hem}} \boldsymbol{Q}\otimes\boldsymbol{Q} dV = \int_0^R\int_0^{2\pi}\int_0^{\pi/2}(\boldsymbol{Q}\otimes\boldsymbol{Q}) r\, d\phi\, r\sin\theta\, d\theta\, dr =$$

$$= \frac{R^3}{3}\frac{1}{\frac{2\pi R^3}{3}}\int_0^{2\pi}\int_0^{\pi/2}(\boldsymbol{Q}\otimes\boldsymbol{Q}) d\phi\ \sin\theta\ d\theta$$

$$= \frac{1}{2\pi}\int_0^{2\pi}\int_0^{\pi/2}(\boldsymbol{Q}\otimes\boldsymbol{Q}) d\phi\ \sin\theta\ d\theta \tag{6}$$

In the above expression the case of fibers randomly distributed in the 3D space has been considered, but the generic case of preferentially oriented fibers can be also treated in a similar way [27].

3. NURBS functions and surfaces

3.1 NURBS basis functions and derivatives

NURBS basis is given by

$$R_i^p(\xi) = \frac{N_{i,p}(\xi)w_i}{W(\xi)} = \frac{N_{i,p}(\xi)w_i}{\sum_{i'=1}^{n} N_{i',p}(\xi)w_{i'}} \tag{7a}$$

where $N_{i,p}(\xi)$ are B-spline basis functions recursively defined by using Cox-de Boor formula and starting with piecewise constants ($p = 0$) [28]

$$N_{i,0}(\xi) = \begin{cases} 1 & if \;\; \xi_i \leq \xi < \xi_{\boldsymbol{i+1}} \\ 0 & otherwise \end{cases} \tag{7b}$$

and for $p = 1,2,3, \dots$

$$N_{i,p}(\xi) = \frac{\xi - \xi_i}{\xi_{i+p} - \xi_i} N_{i,p-1}(\xi) + \frac{\xi_{i+p+1} - \xi}{\xi_{i+p+1} - \xi_{i+1}} N_{i+1,p-1}(\xi) \tag{7c}$$

w_i is also referred to as the i^{th} weight while $W(\xi)$ is weighting function defined as follows:

$$W(\xi) = \sum_{i=1}^{n} N_{i,p}(\xi) w_i \tag{7d}$$

Simply applying the quotient rule to Eq. (7a) yields:

$$\frac{d}{d\xi} R_i^p(\xi) = w_i \frac{W(\xi) N_{i,p}^{'}(\xi) - W'(\xi) N_{i,p}(\xi)}{(W(\xi))^2} \tag{8a}$$

where,

$$N_{i,p}^{'}(\xi) = \frac{p}{\xi_{i+p} - \xi_i} N_{i,p-1}(\xi) - \frac{p}{\xi_{i+p+1} - \xi_{i+1}} N_{i+1,p-1}(\xi) \tag{8b}$$

and

$$W'(\xi) = \sum_{i=1}^{n} N'_{i,p}(\xi) w_i \tag{8c}$$

Among NURBS basis functions characteristics, the most important ones are partition of unity property, compact support of each basis function and non-negative values. It can be also noted that if the weights are all equal, then $R_i^p(\xi) = N_{i,p}(\xi)$; so, B-spline is the special case of NURBS. Details related to higher order derivatives formulations can be found in [28].

3.2. NURBS curves and surfaces

A NURBS curve is defined as:

$$\boldsymbol{C}(\xi) = \sum_{i=1}^{n} R_i^p(\xi) \boldsymbol{B_i} \tag{9a}$$

where $B_i \in R^d$ are control points and $i = 1,2,...,$ number of control points. Similarly, for definition of a NURBS surface, two knot vectors $\mathrm{E} = \{\xi_1, \xi_2, \ldots, \xi_{n+p+1}\}$ and $\mathrm{H} = \{\eta_1, \eta_2, \ldots, \eta_{m+q+1}\}$ (one for each direction) as well as a control net $\boldsymbol{B}_{i,j}$ are required. A NURBS surface is defined as:

$$\boldsymbol{S}(\xi,\eta) = \sum_{i=1}^{n}\sum_{j=1}^{m} R_{i,j}^{p,q}(\xi,\eta)\, \boldsymbol{B}_{i,j} \tag{9b}$$

where $R_{i,j}^{p,q}(\xi,\eta)$ is defined according to the following equation, while $N_{i,p}(\xi)$ and $M_{j,q}(\eta)$ are univariate B-spline basis functions of order p and q corresponding to knot vector E and H, respectively.

$$R_{i,j}^{p,q}(\xi,\eta) = \frac{N_{i,p}(\xi) M_{j,q}(\eta) w_{i,j}}{\sum_{i'=1}^{n}\sum_{j'=1}^{m} N_{i',p}(\xi) M_{j',q}(\eta) w_{i',j'}} \tag{10}$$

4. Definition of the optimization problem

Lots of structural characteristics or responses can be adopted as optimization objectives. As representative examples we can mention weight, stiffness, natural frequencies or a combination of them. Optimization aimed at obtaining structures with minimum strain energy (minimum structural compliance) – which alternatively means maximum structural stiffness – is the most common approach in this field. Nevertheless, though combination of elastic compliance with structural volume or weight constraints is comprehensive for static problems, obtained designs are not essentially optimum considering dynamic behavior of the structure. One important example is represented by vibrating structures to be designed in such a manner to avoid resonance for external excitation loads varying with a given frequency. This goal is usually obtained by maximizing the fundamental eigenfrequency or the gap between two consecutive eigenfrequencies of the structure [29].

In the context of this paper we will just optimize fiber distribution through the structure by definition of single objective function either for pure static loading or free vibration, separately. Extension of this methodology into multi-objective problems, which deals with systematic and concurrent solution of a collection of objective functions, will be straight forward in formulation but not in concept. Typical multi-objective optimization problem consists of a weighted sum of all objective functions combined to a form of single function. Final solution of this function is totally dependent on the allocated weights. On the other hand from the technological point of view, engineers need to know a specific volume fraction for design and manufacturing of a FRC product. Generally there is no single global solution for multi-objective optimization problems and selection of a set of points as a final solution among thousands of possible solutions, requires to develop a comprehensive selection criteria which is behind the scope of this paper. To review the multi-objective optimization methods in engineering, interested readers can refer to [30].

4.1. Objective function and optimization formulation for static problems

Strain energy can be considered as the work done by internal forces through the deformation of the body. In optimization problem we can consider minimization of this energy as the objective function. For the problem with $m-$ load cases we have:

$$U = \sum_{i=1}^{m} \lambda_i U^i \quad \lambda_i > 0 \tag{11}$$

where U and U^i are the total strain energy and elastic strain energy for the i^{th} load case respectively; while λ_i is the weight associated to the strain energy which has been considered equal to unity unless otherwise specified.

The terms U^i can be defined as:

$$U^i = [\sum_{e=1}^{nel} \frac{1}{2} \int_V \boldsymbol{\varepsilon}_{\boldsymbol{e}}^T \boldsymbol{C}_{\boldsymbol{eq}} \, \boldsymbol{\varepsilon}_{\boldsymbol{e}} dV]^i \tag{12}$$

in above equation formulas $\boldsymbol{\varepsilon}_{\boldsymbol{e}}$ is the strain vector associated with element e and $\boldsymbol{C}_{\boldsymbol{eq}}$ is the homogenised elastic tensor of the composite at each point according to Eq. (5), while nel is the number of elements in the structural component being analyzed.

Nodal fiber volume fraction $\varphi_{i,j}$ (the subscripts i and j belong to counterpart control point, $\boldsymbol{B}_{\boldsymbol{i,j}}$) on control points are defined as design variables and fiber distribution is approximated by using NURBS surface (see Eq. (10) and Fig.3) based on formulation provided in 3.2. Every point on parametric mesh space of the design domain will be mapped to geometrical space having two distinguished identification, i.e. geometrical coordinates and fiber volume fraction value. Intrinsically, even using coarse meshes, distribution function described through a NURBS surface is smooth enough to have clear representation with no need to any further image processing technique.

Fiber distribution function $\eta_p(\boldsymbol{x},\boldsymbol{y})$ – which indicates the fiber amount at every design point and will be used for obtaining homogenized mass and stiffness of finite elements – is defined according to the following relationship:

$$\eta_p(\boldsymbol{x},\boldsymbol{y}) = \sum_{i=1}^{n}\sum_{j=1}^{m} R_{i,j}^{p,q}(\xi,\eta)\ \varphi_{i,j} \tag{13}$$

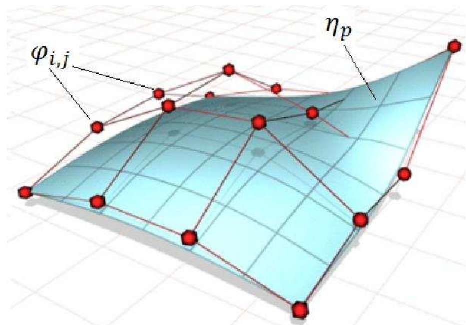

Fig.3. Schematic illustration of fiber distribution function defined by NURBS

Once the fiber volume fraction at each point is available, by substitution in Eq. (5), we can define the equivalent mechanical characteristics of the domain through the following equations:

$$\boldsymbol{C_{eq}}(\boldsymbol{x},\boldsymbol{y}) = \left(1-\eta_p\right)\cdot \boldsymbol{C_m} + \eta_p E_f \cdot \int_V \boldsymbol{Q}\otimes\boldsymbol{Q}\ dV \tag{14}$$

$$\rho(\boldsymbol{x},\boldsymbol{y}) = \left(1-\eta_p\right)\rho_m + \eta_p\rho_f \tag{15}$$

where $\rho(\boldsymbol{x})$ is the equivalent density at every point in the design domain, obtained by using the rule of mixture. ρ_m and ρ_f are matrix material and fiber material density, respectively. The optimization problem can be finally summarized as follows:

Minimize : U

Subjected to : $w_f = \int_V \eta_p\rho_f\, dV \le w_{f0}$ (16)

$$\boldsymbol{Ku} = \boldsymbol{f} \tag{17}$$

$$\varphi_{i,j} - 1 \le 0 \tag{18}$$

$$-\varphi_{i,j} \le 0 \tag{19}$$

where w_f is the total fiber weight in every optimization iteration and w_{f0} is an arbitrary initial fiber weight which must be set at the beginning of the optimization process. $\boldsymbol{K}$, $\boldsymbol{u}$ and $\boldsymbol{f}$ in Eq. (17) (which represent the general system of equilibrium equations in linear elastic finite elements method) are the global stiffness matrix of the system, the displacement and the force vector, respectively.

By introducing a proper Lagrangian objective function, l, and by using the Lagrangian multipliers method we have:

$$l = U - \left(w_f - w_{f0}\right) - \sum_{i,j=1}^{ncp} \psi_1\left(\varphi_{i,j} - 1\right) - \sum_{i,j=1}^{ncp} \psi_2\left(-\varphi_{i,j}\right) \tag{20}$$

where ψ_1, ψ_2 are upper and lower bounds Lagrange multipliers while ncp is the number of control points. By setting the first derivative of Eq. (20) to zero we will obtain:

$$\frac{\partial l}{\partial \varphi_{i,j}} = \frac{\partial U}{\partial \varphi_{i,j}} - \frac{\partial w_f}{\partial \varphi_{i,j}} - \psi_1 + \psi_2 = 0 \tag{21}$$

Eq. (21) can be solved numerically by using different approaches such as the so-called method of moving asymptotes (MMA) algorithm (Svanberg, 1987 [31]). In this work we have implemented optimality criteria (OC) based optimization (Zhou & Rozvany, 1991, [32]) that represents a simple tool to be implement and allows a computationally efficient solution because updating of each design variables takes place independently. We ignore to describe the updating scheme of OC which is based on sensitivity analysis performed in 4.3. However, interested readers can refer to [32] for more details.

4.2. Objective function and optimization formulation for free vibration problems

Maximization of fundamental eigenvalue, which is herein considered as objective function for free vibration problems, can be formulated as follows:

Maximize : ϖ_{min}

Subjected to : $w_f = \int_V \eta_p \rho_f \, dV \leq w_{f0}$ (22)

$(\boldsymbol{K} - \varpi_i \boldsymbol{M})\boldsymbol{\phi_i} = \boldsymbol{0} \qquad i = 1, \ldots, no.of\ DOF$ (23)

$\varphi_{i,j} - 1 \leq 0$ (24)

$-\varphi_{i,j} \leq 0$ (25)

where ϖ_i stands for the i^{th} eigenvalue, ϖ_{min} is the fundamental frequency of the structure, $\boldsymbol{M}$ is the system mass matrix and $\boldsymbol{\phi_i}$ is the eigenvector associated with the i^{th}

eigenfrequency. Eq. (23) represents the standard elastodynamic formulation for free vibration problems without damping.

4.3. Sensitivity analysis

Basically, in order to update design variables toward the optimized solution, OC needs to determine how different values of the independent variable (i.e. $\varphi_{i,j}$) influence the objective function under a given set of design constraints. One method to do this is to consider the partial derivative of the objective function and constraints with respect to design variables.

In Eq. (21) we can calculate $\frac{\partial U}{\partial \varphi_{i,j}}$ and $\frac{\partial w_f}{\partial \varphi_{i,j}}$ through the following expressions:

$$\frac{\partial U}{\partial \varphi_{i,j}} = \sum_{i=1}^{m} \lambda_i \frac{\partial U^i}{\partial \varphi_{i,j}} \tag{26}$$

where

$$\frac{\partial U^i}{\partial \varphi_{i,j}} = \frac{1}{2} \int_V \boldsymbol{\varepsilon}^T \frac{\partial \boldsymbol{C_{eq}}}{\partial \varphi_{i,j}} \boldsymbol{\varepsilon} \, dV \tag{27}$$

while

$$\frac{\partial \boldsymbol{C_{eq}}}{\partial \varphi_{i,j}} = -\frac{\partial \eta_p}{\partial \varphi_{i,j}} \cdot \boldsymbol{C_m} + \frac{\partial \eta_p}{\partial \varphi_{i,j}} E_f \cdot \int_V \boldsymbol{Q} \otimes \boldsymbol{Q} \, dV \tag{28}$$

and

$$\frac{\partial \eta_p}{\partial \varphi_{i,j}} = R_{i,j}^{p,q}(\xi, \eta) \tag{29}$$

It should be declared that in order to calculate Eq. (28), the value $\frac{\partial \boldsymbol{C_m}}{\partial \varphi_{i,j}} = 0$ has been considered since the Poisson's ratios for both fiber and matrix are assumed to be the same. On the other hand $\frac{\partial w_f}{\partial \varphi_{i,j}}$ can be also calculated as follow:

$$\frac{\partial w_f}{\partial \varphi_{i,j}} = \int_V \frac{\partial \eta_p}{\partial \varphi_{i,j}} \rho_f \, dV \tag{30}$$

For the problem of free vibration, we follow the same procedure in order to perform sensitivity analysis; So we calculate partial derivatives of each term of Eq. (23) with respect to $\varphi_{i,j}$:

$$\left(\frac{\partial \boldsymbol{K}}{\partial \varphi_{i,j}} - \frac{\partial \varpi_i}{\partial \varphi_{i,j}} \boldsymbol{M} - \varpi_i \frac{\partial \boldsymbol{M}}{\partial \varphi_{i,j}}\right) \boldsymbol{\phi_i} = 0 \tag{31}$$

by rewriting Eq. (31) and normalizing eigenvector with respect to the kinetic energy (i.e. $\boldsymbol{\phi_i}^T \boldsymbol{M}\, \boldsymbol{\phi_i} = 1$) , we will finally have:

$$\frac{\partial \varpi_i}{\partial \varphi_{i,j}} = \boldsymbol{\phi_i}^T \left(\frac{\partial \boldsymbol{K}}{\partial \varphi_{i,j}} - \varpi_i \, \frac{\partial \boldsymbol{M}}{\partial \varphi_{i,j}}\right) \boldsymbol{\phi_i} \tag{32}$$

where:

$$\frac{\partial \boldsymbol{K}}{\partial \varphi_{i,j}} = \int_V \boldsymbol{B}^T \frac{\partial \boldsymbol{C_{eq}}}{\partial \varphi_{i,j}} \boldsymbol{B}\, dV \tag{33}$$

and $\boldsymbol{B}$ is the standard finite element compatibility matrix containing the derivatives of the shape functions while $\frac{\partial \boldsymbol{C_{eq}}}{\partial \varphi_{i,j}}$ can be obtained through Eq. (28). Derivative of consistent mass matrix with respect to design variables can be calculated as follows:

$$\frac{\partial \boldsymbol{M}}{\partial \varphi_{i,j}} = \int_V \boldsymbol{N}^T \frac{\partial \rho}{\partial \varphi_{i,j}} \boldsymbol{N} dV \tag{34}$$

while:

$$\frac{\partial \rho}{\partial \varphi_{i,j}} = -\frac{\partial \eta_p}{\partial \varphi_{i,j}} \rho_m + \frac{\partial \eta_p}{\partial \varphi_{i,j}} \rho_f \tag{35}$$

in Eq. (34) $\boldsymbol{N}$ is the matrix of shape functions while $\frac{\partial \eta_p}{\partial \varphi_{i,j}}$ can be calculated by Eq. (29).

4.4. Optimization procedure

In the present optimization procedure, after definition of the optimum problem according to Sections 4.1 and 4.2, once discretized the structural element domain through finite elements, the obtained discrete model is analyzed based on the considered design parameters (i.e. geometry, loading, boundary conditions, material constraints, …), starting from the initial value of the design variable (i.e. available fiber volume fraction). Afterwards the optimizer does sensitivity analysis (as explained in Section 4.3) and then OC updates design variables. This computational procedure is performed iteratively till no sensible changes (limit can be set as a design parameter) occur in design variables. Fig. 4 summarizes this procedure.

It is also worth noting that NURBS basis functions have dual application in the present work: fiber distribution and model analysis. The latter, has been followed by quadratic

NURBS finite elements through an isogeometric analysis (IGA) approach. Interested readers can refer to [28] and references therein to know more about IGA.

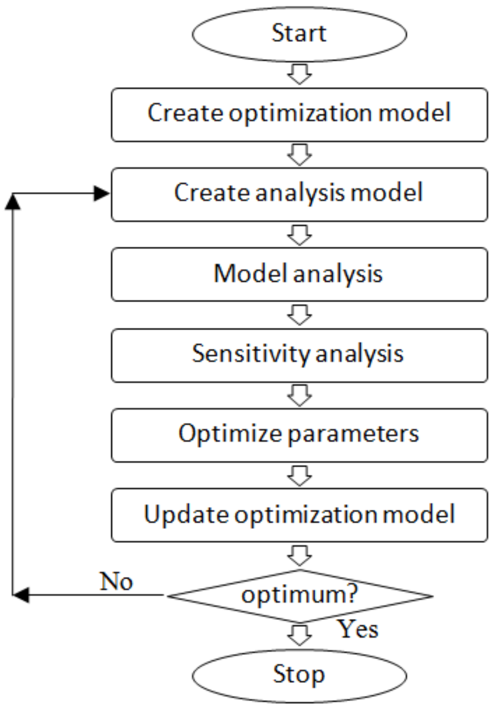

Fig.4. Optimization algorithm

5. Numerical examples

In this section the applicability and reliability of the model has been investigated by conducting some numerical examples in order to demonstrate the advantages of the proposed optimization model.

In the present algorithm the minimum and the maximum values of fiber content in each design point can be set by designer before optimization process commencement. For the case of random distribution of fiber in the matrix, the maximum fiber content practically can range between 30%-60%. The minimum value of the fiber content has been also considered 0.1 % through this paper unless otherwise specified.

5.1 Three-point bending of a wall beam

The first example involves a three point bending problem of a plane stress wall beam. Schematic view and design parameters are as shown in Fig.5 and Table-1, respectively.

We considered a constant total fiber volume fraction equal to 10% and solved the optimization problem to find the optimum distribution of fibers in the wall beam to obtain minimum structural elastic compliance. Fig. 6 (a) shows result of fiber distribution optimization in half of the wall beam. Regions with white color stand for minimum fiber content (which is set equal to 0.1 %), while black regions depict maximum fiber content and gray regions have the value between minimum and maximum.

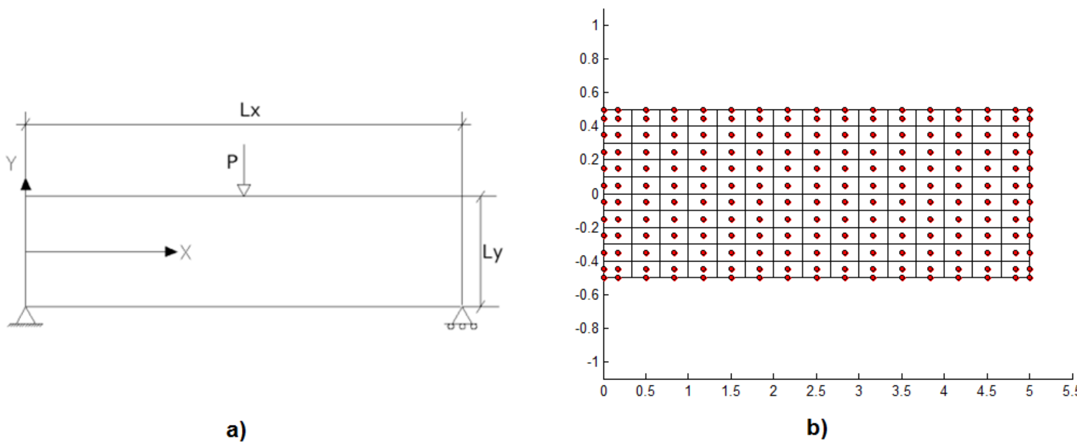

Fig.5. Geometry (a) and FE mesh with control points indicated by dots (b) of a three-point bending wall beam

Table 1. Problem definitions, wall beam under three-point bending

L_x	L_y	E_m	E_f	ν	ρ_m	ρ_f	P	V_f	V_{fmax}	No. control points
5	1	20	200	0.1	1000	1450	1000	10%	60% & 30%	$22 \times 12 = 264$

$Length: m,\ \ E: GPa\ ,\ \ P: Applied\ load\ (N),\ \ \nu: Poisson\ ratio,\ \ \rho: density\ \left(\frac{kg}{m^3}\right), m: matrix, f: fiber$

$V_f\ :fiber\ volume\ fraction,\qquad V_{fmax}\ :maximum\ fiber\ volume\ fraction,$

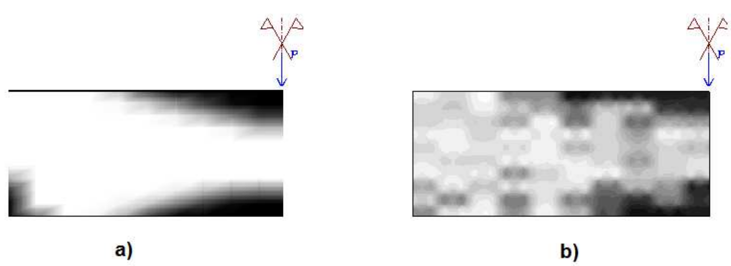

Fig.6. Optimized fiber distribution through left half of the beam (a) current methodology and (b) ref.[18]

Fig. 6 (b) shows the benchmark result as presented in [18]. Using the same number of elements for both (a) and (b), although there are some local differences which can be mainly referred to the heuristic nature of GA and element based demonstration of results used in [18], one can figure out the general conformity between two categories of results since in both results, fibers are more concentrated on regions under the loaded point, regions with maximum displacements and around supports. Readers should also notice that this comparison is just for general verification of the presented method not for detail adaptation. This is due to the fact that both categories of results are slightly dependent to setting of their variables (initial populations, probability of cross over, probability of mutation for results of [18] and maximum fiber volume fraction, end point of optimization algorithm, solution tolerance for the present work).

Fig.7 (a) shows the obtained results for the case that maximum fiber content in each design point is allowed to be increase up to 60%, while for the case (b) this value is assumed to be equal to 30%. Results provided by subsequent optimization iterations are shown from top to bottom; as expected, by decreasing the upper limit of local fiber content, the obtained fiber layout occupies more area of admissible design domain while total used fibers is the same for (a) and (b). Having assumed a constant total fiber volume fraction and considering different admissible values for maximum fiber content in each element, normalized elastic compliance (using 264 control points) versus the number of iterations are accordingly plotted in Fig.8. High rate and smooth convergence can be appreciated; these desirable computational characteristics have been obtained thanks to both implemented methodologies (particularly optimization based on sensitivity analysis instead of heuristic method) and NURBS finite elements. It is also noteworthy to point out that, by increasing maximum admissible fiber volume in each element, lower compliance will be obtained. This simply can be explained by considering that, increasing maximum admissible fiber volume will cause fibers to gather up more and more in the most appropriate design points having the highest influence on increasing the structural stiffness, not in somewhere around the best points.

Readers should distinguish between the so called “fiber gathering up” and “fiber agglomeration”. The former, which stands for increase in fiber volume fraction, happens in structural design domain (i.e at the macro scale) but the latter, basically is addressed in

RVE scale. Moreover in contrary with agglomeration which reduces the structural stiffness (in comparison with uniformly distributed fibers), optimum fiber distribution always yields to an increase in structural stiffness.

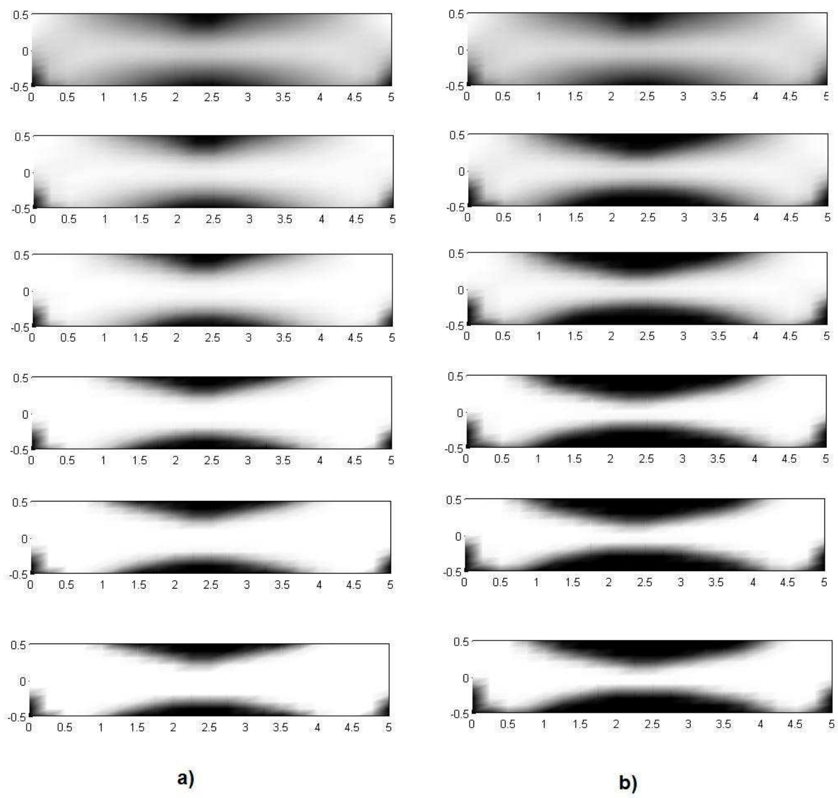

Fig.7. Optimum fiber distribution in beam considering a constant total fiber volume equal to 10%; the maximum local fiber content is assumed equal to (a) 60% and (b) 30%; iterations results are displayed from top to bottom for each case

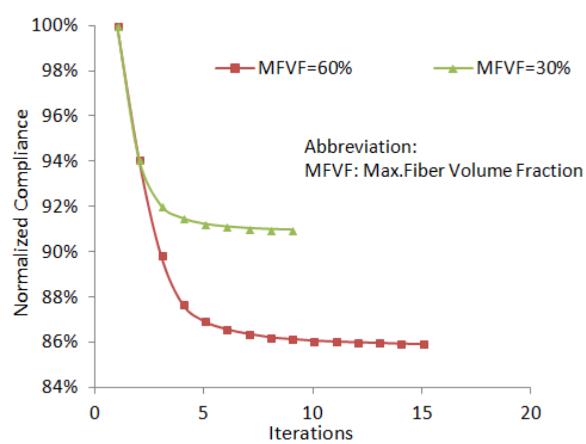

Fig.8. Normalized compliance versus number of iterations for different values of maximum fiber content in each element, using 264 control points (MFVF: maximum fiber volume fraction)

5.2 Free vibration of a beam

In the second example free vibration of a FRC beam under different support conditions has been considered. As indicated in Fig.9 a cantilever beam (Fig. 9(a)) and a clamped beam (Fig. 9(b)) have been assumed. Design parameters are according to Table-2 and FE discretization is the same as in the previous example.

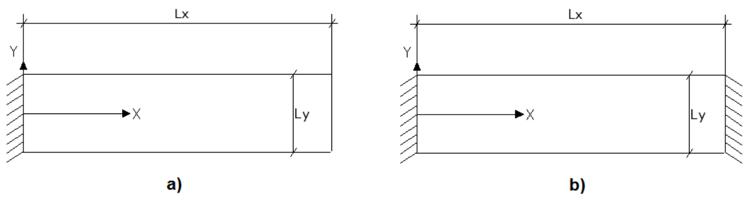

Fig. 9. Schematic view of problem geometry, a) cantilever beam b) clamped beam

Table 2. Problem definitions, free vibration of a beam

L_x	L_y	E_m	E_f	ν	ρ_m	ρ_f	V_f	V_{fmax}	No. control points
5	1	20	200	0.1	1000	1450	10%	60%	$22 \times 12 = 264$

$Length: m,\ \ E: GPa\ ,\ \ \nu: Poisson\ ratio,\ \ \rho: density\ \left(\frac{kg}{m^3}\right), m: matrix, f: fiber$

$V_f\ : fiber\ volume\ fraction,\qquad V_{fmax}\ : maximum\ fiber\ volume\ fraction$

In this problem the adopted objective function aims to get the maximum value of the fundamental frequency by optimizing fiber distribution through the beam domain. First modal shape as well as fiber distribution optimization results for both cantilever and clamped beams are demonstrated in Fig.10 (a, b), respectively.

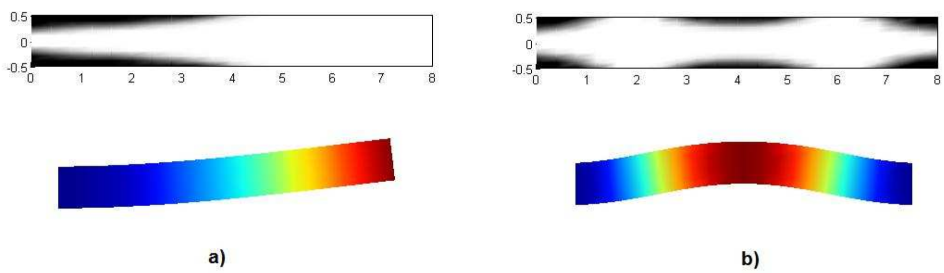

Fig. 10. First modal shapes and optimum fiber distribution for a cantilever beam (a) and a clamped beam (b)

Fig. 11 shows the patterns of the objective function (fundamental frequency of the beam normalized with respect to the case of uniformly reinforced material) versus the optimization iterations. It can be observed as the increasing in fundamental frequencies are around 11% for cantilever and 7% for clamped beams.

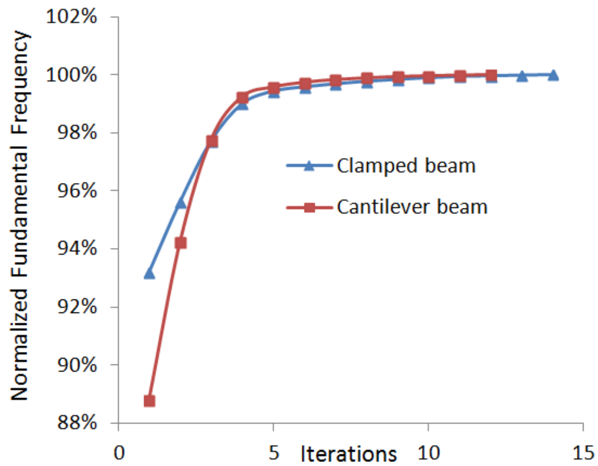

Fig. 11. Normalized fundamental frequency versus iterations for beam with different supporting conditions

5.3 Square plate with a central circular hole under tension

As the third example, a square plate with central hole under constant distributed edge load was studied. Due to the double symmetry only one quarter of this plate is modeled. Fig.12 (a, b) and Table-3 show analysis model, the FE domain discretization and the design parameters, respectively. The problem of obtaining minimum elastic compliance (objective function) is solved by using quadratic NURBS meshes.

Table 3. Problem definitions, plate with a central circular hole under tension

L	R	E_m	E_f	ν	ρ_m	ρ_f	p	V_{fmax}	No. control points
4	1	20	200	0.1	1000	1450	510	60%	180, 612, 2244

$Length: m,\ \ E: GPa\ ,\ \ \mathbf{p}: Load\ (N/m),\ \ \nu: Poisson\ ratio,\ \ \rho: density\ \left(\frac{kg}{m^3}\right), m: matrix, f: fiber$

$V_{fmax}\ \ : maximum\ fiber\ volume\ fraction$

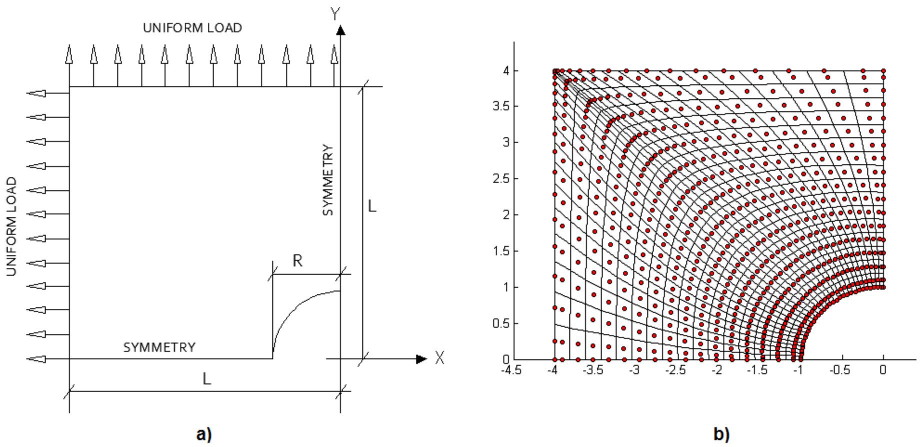

Fig. 12. a) Schematic view of the model under uniform edges load ***p*** and b) mesh with control points (dots)

Fig.13 presents optimum fiber distribution through the structure. Results represented in Fig. 13(a, b, c) correspond to meshes with 180, 612 and 2244 control points, respectively; as can be observed, smooth solution can be also obtained not necessarily by implementing fine meshes.

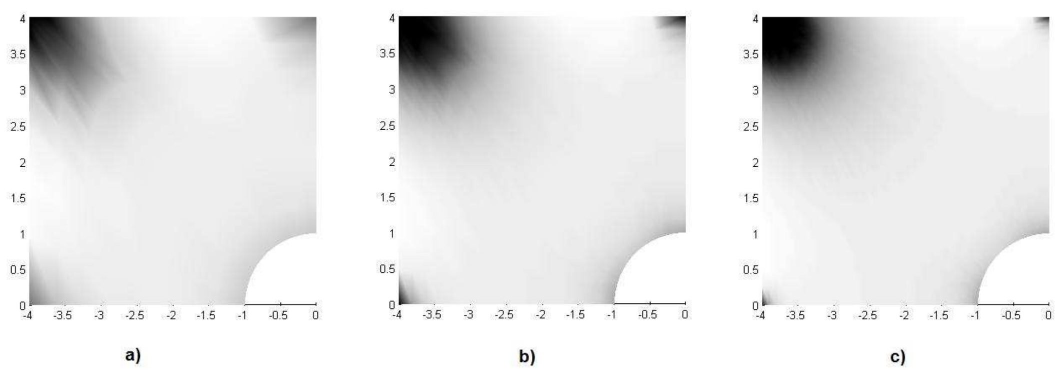

Fig. 13. Optimum fiber distribution using (a) 180 control points, (b) 612 control points and (c) 2244 control points

Histories of objective function (normalized elastic compliance) versus the iteration steps for different mesh sizes are plotted in Fig.14; it can be noted as the deviation between results less than 2% can be obtained by using coarse meshes with respect to the finer one, while computational cost is obviously lower by using rough discretization. On the other words, the use of coarse NURBS mesh maintains precision of the results while decreasing the computational time.

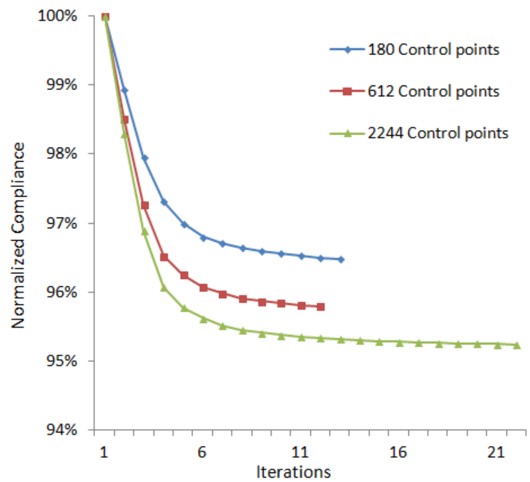

Fig. 14. Normalized compliance versus number of iterations for different mesh sizes

6. Conclusions

The efficient gradient based optimization of fiber distribution in fiber reinforced continuum elements, has been developed in the present paper through the use of NURBS functions. The adopted computational technique has been implemented and used for both domain discretization and definition of fiber distribution function. The proposed approach allows to get a high rate and smooth convergence to the optimum condition sought while results are also mesh independent. The method allows considering generic objective functions. In particular in the present research the minimization of elastic strain energy and maximization of fundamental frequency for static and free vibration problems have been considered respectively; by varying the fibers distribution characteristics in the body under study. Nodal volume fraction of fiber has been used as the optimization design variable, whose distribution function has been smoothly approximated by using a NURBS surface. The mechanical behavior of the composite has been macroscopically described through a homogenization approach based on random orientation of fibers in the matrix. Some representative numerical examples have finally been presented; both optimization related to the structural response under static loading and the free vibration behavior of composite structural elements, have been considered and demonstrated that combining NURBS approximation and sensitivity based optimization method yields to high convergence rate and mesh independent optimization results.

Acknowledgments:

This work was supported partially by Marie Curie Actions under the grant IRSES-MULTIFRAC and German federal ministry of education and research under the grant BMBF SUA 10/042. Nachwuchsförderprogramm of Ernst Abbe foundation, the National Basic Research Program of China (973 Program: 2011CB013800), Program for Changjiang Scholars and Innovative Research Team in University (PCSIRT, IRT1029) and Pujiang Program (12PJ1409100) and the research support provided by the Italian Ministry for University and Technological and Scientific Research (MIUR) are also acknowledged.

References:

[1] F.S. Almeida, A.M. Awruch, Design optimization of composite laminated structures using genetic algorithms and finite element analysis, Composite Structures 88 (2009) 443-454.

[2] M. Kemal Apalak, Mustafa Yildirim, Layer optimization for maximum fundamental frequency of laminated composite plates for different edge conditions, Composite Structures 68 (2008) 537-550.

[3] Taeseong Kim, Jaehoon Lim, Structural design optimization of a tiltrotor aircraft composite wing to enhance whirl flutter stability, Composite Structures 95 (2013) 283-294.

[4] D.S. Lee, C. Morillo, Multilayered composite structure design optimization using distributed/parallel multi-objective evolutionary algorithms, Composite Structures 94 (2012) 1087-1096.

[5] Gyeong-Chan Lee, Jin-Hwe Kweon, Optimization of composite sandwich cylinders for underwater vehicle application, Composite Structures 96 (2013) 691-697.

[6] S.N. Omkar, Dheevatsa Mudigere, Vector evaluated particle swarm optimization (VEPSO) for multi-objective design optimization of composite structures, Computers and Structures 86 (2008) 1-14.

[7] N. Zehnder, P. Ermanni, A methodology for the global optimization of laminated composite structures, Composite Structures 72 (2006) 311-320.

[8] R. S. Salzar, Functionaly graded metal matrix composite tubes, Composite Eng. 5 (1995) 891-900.

[9] J.C. Nadeau, M. Ferrari, Microstructural optimization of a functionally graded transversely isotropic layer, Mechanics of Materials 31 (1999) 637-651.

[10] Shinya Honda, Yoshihiro Narita, Vibration design of laminated fibrous composite plates with local anisotropy induced by short fibers and curvilinear fibers, Composite Structures 93 (2011) 902-910.

[11] Senthil Murugan, Erick I. Saavedra Flores, Optimal design of variable fiber spacing composites for morphing aircraft skins, Composite Structures 94 (2012) 1626-1633.

[12] Kulasegaram S, Karihaloo BL, Ghanbari A, Modelling the flow of self-compacting concrete, International Journal for Numerical and Analytical Methods in Geomechanics , 35 (6) (2011) 713-723 ISSN 0363-9061 10.1002/nag.924

[13] Kulasegaram S, Karihaloo BL, Fibre-reinforced, self-compacting concrete flow modelled by smooth particle hydrodynamics, Proceedings of the ICE Engineering and Computational Mechanics , 166 (1) (2012) 22-31 ISSN 1755-0777 10.1680/eacm.11.00004

[14] J. Huang, R.T. Haftka, Optimization of fiber orientations near a hole for increased load-carrying capacity of composite laminates, Struct Multidisc Optim. 30 (2005) 335-341.

[15] Brighenti R., Optimum patch repair shapes for cracked members, Int. J. of Mech. Mat. in Des. 1(4) (2004) 365-381.

[16] Brighenti R, Carpinteri A, Vantadori S, A., genetic algorithm applied to optimization of patch repairs for cracked plates, Comp. Meth. App. Mech. Eng 1960 (2006) 466-475.

[17] Brighenti R., Patch repair design optimization for fracture and fatigue improvements of cracked plates, J. of Sol. Struct. 44(3-4) (2007) 1115-1131.

[18] R. Brighenti, Fiber distribution optimization in fiber-reinforced composites by a genetic algorithm, Composite Structures 71 (2005) 1-15.

[19] Hashin Z., The elastic moduli of heterogeneous materials, J Appl Mech. 29 (1962) 143-150.

[20] Hashin Z. and S. Shtrikman, A variational approach to the theory of elastic behavior of multiphase materials, J. Mech. Phys. Solids 11 (1963) 127-140.

[21] B.Paul, Prediction of elastic constants of multiphase materials, Transactions of the Metallurgical Society of AIME (1960) p. 36-41.

[22] Hill R., A self-consistent mechanics of composite materials, J. Mech. Phys. Solids 13 (1965) 213-222.

[23] Mori T, Tanaka K., Average stress in matrix and average elastic energy of materials with mis-fitting inclusions, Acta Metal 21 (1973) 571-583.

[24] R. Brighenti, A mechanical model for fiber reinforced composite materials with elasto-plastic matrix and interface debonding, Int. J. of Computational Materials Science 29 (2004) 475-493.

[25] R. Brighenti, A micromechanical model and reinforcing distribution optimization approach for fiber-reinforced materials. In: Qingzheng (George) Cheng (ed) Fiber Reinforced Composites, Nova Science Publishers, Inc., Hauppauge, NY, 2012, pp. 527-569.

[26] R. Brighenti, Numerical modeling of the fatigue behavior of fiber-reinforced composites, Int. J. of Composite Part B: Engineering 35(3) (2004) 197-210.

[27] R. Brighenti, D. Scorza, A micro-mechanical model for statistically unidirectional and randomly distributed fiber-reinforced solids, Mathematics and Mechanics of Solids 17(8) (2012) 876–893.

[28] J.A. Cottrell, T.J.R. Hughes, Y.Bazilevs, Isogeometric Analysis towards integration of CAD and FEA, Wiley, UK, 2009.

[29] Du J., Olhoff N., Topological design for freely vibrating continuum structures for maximum values of simple and multiple eigenfrequencies and frequency gaps, Struct multidisc opt. 34 (2007) 91-110.

[30] R.T.Marler, J.S. Arora, Survay of multi-objective optimization methods for engineering, Struct multidisc opt. 26 (2004) 369-395.

[31] Svanberg K., The method of moving asymptotes- a new method for structural optimization, Int. J. of Numerical Methods in Eng. 24 (1987) 359-373.

[32] Zhou M., Rozvany GIN, The COC algorithm part II: topological, geometry and generalized shape optimization, Comput. Methods Appl. Mech. Eng. 89 (1991) 197-224.